

Energy partitioning and particle spectra in multicomponent collision cascades

Martin Vicanek, Ulrich Conrad, and Herbert M. Urbassek

Institut für Theoretische Physik, Technische Universität, W-3300 Braunschweig, Germany

(Received 18 March 1992; revised manuscript received 19 August 1992)

Energy distributions of recoil atoms in collision cascades in composite media are studied analytically. The pertinent integral transport equations are reduced to a computationally much simpler system of differential equations. This is possible for arbitrary particle interaction potentials. The accuracy of this transformation is demonstrated by comparison with Monte Carlo computer simulation. As a case study, energy partitioning among the target species in a collision cascade in the (hypothetical) binary compound $\text{Hf}_x\text{C}_{1-x}$ is investigated. We find that the number of recoils produced is understoichiometric for both species. On the other hand, the particle flux of the lighter species is overstoichiometric, while the flux of the heavy species shows only small deviations from stoichiometry. The energy is deposited preferentially in low-energy recoil motion of the lighter species. Reference is made to earlier theoretical treatments of the problem for less-general-interaction cross sections. The differences found are mainly quantitative, and their origin is traced back partly to the differences in the physical input, and partly to the restricted validity of the previous methods. Energy spectra of particles sputtered from a compound are studied, concentrating on an experiment on HfC sputtering. We find, in agreement with the experiment, that Hf and C species show similar slopes. We predict that energy spectra from diluted compounds will show larger differences in their slopes.

I. INTRODUCTION

The theoretical description of energetic particle slowing down and recoil generation is of a long standing in theoretical physics.¹ The energy distribution of recoils generated in a collision cascade can be determined from so-called transport equations. These are linear integral equations, which contain the particle interaction cross sections as their essential ingredients. The analytical solution of these equations is known only for rather special interaction cross sections.^{2,3} We present in this paper a general method to calculate energy distributions in collision cascades. This method may be used for arbitrary interaction cross sections. It consists of approximating the transport integral equations by a system of ordinary differential equations that are considerably easier to solve. We check the validity of our approach by comparison with computer simulation results.

While asymptotic energy distributions of recoil atoms in a monoatomic medium have been studied long ago with sufficient care,^{2,3} the recoil particle distributions in multicomponent media are not known in the general case. The study by Andersen and Sigmund⁴ is based on a restricted class of power-law interaction cross sections. An analysis with more general, but still power-law cross sections has been carried out in Ref. 5, where two of us rigorously derived the asymptotic energy distributions and also presented comparisons to Monte Carlo simulations. The general case of energy sharing in a multicomponent cascade was classified into three limiting regimes:⁵ (i) a situation of *detailed balance*, where each species receives as much energy from the others as it returns to them; (ii) a regime called *dominance*, where one species will determine the behavior, and the other species adopts the characteristics of the first species particle spectra; (iii)

a case of *ignorance*, where each species behaves as if the other were not present. The results of Ref. 4 fall into the class of detailed balance.

The above classification strictly applies only to the asymptotic stage of the cascade. Realistic collision cascades, in contrast, do not show such a clearcut behavior, partly because the asymptotics is reached only at very small energies, which fall outside the range of validity of the model, and partly because the interaction cross section is not well described by a single power.

Generalization of the above calculations to arbitrary cross sections is not feasible with those methods. In this paper, we present a new analytical method to evaluate the energy distributions of recoils in compound targets for general cross sections. In particular, the results of Ref. 4 are recovered as a special case. The differences in the results brought about by the use of a more realistic interaction law are shown to be significant.

The problem of energy partitioning in a collision cascade is of interest for the question of damage production and recoil generation in compound media.^{4,6-9} From a materials science point of view, an answer to this question requires the knowledge of a number of parameters such as the displacement threshold and bulk binding energies of atoms of each species in the compound. These quantities are not always well known. Moreover, they may vary with the concentrations in the compound. In the present study, we will consider the displacement thresholds as known and disregard all binding energies. Hence our main topic is the deviation from stoichiometry of damage production and recoil generation.

A further example where the present analysis may attract attention is the study of preferentiality in compound sputtering. Of course, the absolute magnitude of the sputter yield of each species depends strongly on the

respective surface binding energy. Again, as these quantities are poorly known, we will not discuss the absolute magnitude of sputter preferentiality. However, the issue was raised that the *energy spectrum* may be different for the individual particle species sputtered from a compound;¹⁰ experimental tests have not verified this prediction.^{11,12} A recent theoretical study⁵ based on power-law interaction potentials clarified this discrepancy and pointed out that in the cases investigated experimentally, a situation of detailed balance between the species will be established in which the energy spectra of the species show a similar slope. We will take up this issue again in this work, and generalize the previous statement to arbitrary collision cross sections.

II. DERIVATION OF APPROXIMATE TRANSPORT EQUATIONS

Consider a homogeneous medium of atomic density N , which consists of n different species of atomic fraction c_i ($i=1, \dots, n$) and mass M_i . Let a fast particle of species $n=1$, which has at time $t=0$ energy $E=E_0$, slow down in this medium, thereby initiating in it a collision cascade. Let furthermore $f_i(E, t)dE$ denote the number of particles of species i with energy between E and $E+dE$ at time t .

The collision cross section of an i particle of energy E to scatter at a j atom at rest and lose an energy between T and $T+dT$ is denoted by

$$d\sigma_{ij} = \sigma_{ij}(E, T)dT. \quad (1)$$

The maximum possible energy transfer is determined from kinematical reasons to be

$$T_{\max} = \gamma_{ij}E, \quad \gamma_{ij} = \frac{4M_iM_j}{(M_i+M_j)^2}. \quad (2)$$

The time evolution of the particle distributions f_i may be described by using so-called transport equations;^{1-3,10,5} these will be employed in this work in their forward form. They read

$$N \sum_j \int dT \{ c_j \sigma_{ij}(E+T, T) \Psi_i(E+T) + c_i \sigma_{ji}(E+T, E) \Psi_j(E+T) - c_j \sigma_{ij}(E, T) \Psi_i(E) \} + \delta_{i1} \delta(E-E_0) = 0. \quad (3)$$

Here we have introduced the time integrated particle fluxes Ψ_i ,

$$\Psi_i(E) = \int_0^\infty dt v_i f_i(E, t), \quad (4)$$

where v_i is the velocity of the i atom with energy E , $v_i = \sqrt{2E/M_i}$. Furthermore, $\delta(x)$ denotes Dirac's delta function, and δ_{i1} equals 1 if $i=1$, and 0 otherwise. Thus, Eq. (3) allows to compute the fluxes $\Psi_i(E)$ for each species i in a cascade initiated by the species $i=1$ with energy E_0 . We note that the case of bombardment with a species different from the target constituents may be formally included here by setting $c_1=0$.

It is useful to introduce the balance of collisions ap-

pearing in Eq. (3)

$$\Delta_i(E) = N \sum_j \int dT \{ c_j \sigma_{ij}(E+T, T) \Psi_i(E+T) + c_i \sigma_{ji}(E+T, E) \Psi_j(E+T) - c_j \sigma_{ij}(E, T) \Psi_i(E) \}. \quad (5)$$

We shall refer to the first term as the scatter term, the second as the recoil term, and the third as the loss term. With the balance of collisions Δ_i , the transport equations (3) simply read

$$\Delta_i(E) + \delta_{i1} \delta(E-E_0) = 0. \quad (6)$$

We wish to solve Eq. (3) approximately for $E \ll E_0$. This is done by a Taylor expansion of the integrand in the balance of collisions Δ . We give the details of this expansion in Appendix A. It may be noted that the analysis is in the spirit of the so-called *age theory* introduced in neutron and electron-transport theory.^{13,14} As a result, the set of integral equations (3) is transformed to a system of differential equations

$$N \sum_j [-c_j S_{ij}(E) \Psi_i(E) + c_i S_{ji}(E) \Psi_j(E)] + \frac{d}{dE} N \sum_j [c_j \sigma_{ij}^s(E) E^2 \Psi_i(E) + c_i \sigma_{ji}^r(E) E^2 \Psi_j(E)] + E \delta_{i1} \delta(E-E_0) = 0, \quad (7)$$

with the obvious initial condition $\Psi_i(E > E_0) = 0$. In Eq. (7), the stopping cross sections S_{ij} and the (partial) energy slowing down cross sections σ_{ij}^s and σ_{ij}^r have been introduced:

$$S_{ij}(E) = \int_0^{T_{\max}} dT T \sigma_{ij}(E, T), \quad (8)$$

$$\sigma_{ij}^s(E) = - \int_0^{T_{\max}} dT \left[1 - \frac{T}{E} \right] \ln \left[1 - \frac{T}{E} \right] \sigma_{ij}(E, T), \quad (9)$$

$$\sigma_{ij}^r(E) = - \int_0^{T_{\max}} dT \frac{T}{E} \ln \frac{T}{E} \sigma_{ij}(E, T). \quad (10)$$

In Appendix B we evaluate these moments for Kr-C interaction.

Let us pause for a moment to contemplate the differences brought about in our asymptotic expression for the balance of collisions from the rigorous integral expression (3). Rigorously, we need to know the fluxes Ψ_j in an interval of energies above E in order to determine the balance of collisions Δ_i at energy E . In contrast, in our asymptotic expression, only *local* properties of the fluxes Ψ_j at the very energy E are needed. The terms in Eq. (7) may be interpreted in the following way: The first term, $-c_j S_{ij} \Psi_i$, denotes the rate at which i atoms scatter out of the energy interval (E, dE) ; in this term the net effect of scattering of i particles into the energy interval (E, dE) due to the slowing down from higher energies is taken into account. The second term, $+c_i S_{ji} \Psi_j$, describes the generation rate of i recoils in the energy inter-

val (E, dE) due to j atoms colliding at higher energies with i atoms at rest. The term containing an energy derivative is less obvious than the other two. In Sec. III, we will identify it as the derivative of the so-called energy slowing down density.

In a monoatomic medium, this last term is the only one contributing, since the other two cancel identically. Conversely, in a situation of detailed balance, the third term is unimportant against the first and second. We will discuss this case further in Sec. V C.

III. ENERGY SLOWING DOWN DENSITY AND DEPOSITED ENERGY

Before discussing the validity of the analysis performed above and the solutions of the resulting equations, it is useful to study its relation to the so-called energy slowing down density. This motivates the name "energy slowing down cross sections" given to the quantities $\sigma_{ij}^s, \sigma_{ji}^r$, Eqs. (9) and (10), and will shed more light on the analysis itself.

Let us introduce the energy slowing down density $\omega(E)$, first in a monoatomic medium. It is defined as the average amount of energy dissipated through collisions from particles moving with energy $E' > E$ down to energies below E . This may happen either by generating a recoil with energy $T < E$, or by losing in a collision a sufficient amount of energy T , so that the remaining energy $E' - T$ falls below E . Thus, in a monoatomic medium, it is

$$\omega_i(E) = N \sum_j \int_E^{E_0} dE' \left[\Psi_j(E') c_i \int_0^E \sigma_{ji}^s(E', T) T dT + \Psi_i(E') c_j \int_{E'-E}^{E'} \sigma_{ij}^r(E', T) (E' - T) dT \right]. \quad (13)$$

We note that Williams¹⁵ uses a definition for the energy slowing down density, which coincides with Eq. (11) for the case of a monoatomic medium, but is different from Eq. (13) for the general case.

Taking the derivative of Eq. (13) with respect to E , one obtains, in analogy to Eq. (12)

$$-\frac{d\omega_i}{dE} + N \sum_j [\Psi_i(E) c_j S_{ij}(E) - \Psi_j(E) c_i S_{ji}(E)] = E \delta_{i1} \delta(E - E_0). \quad (14)$$

This equation is readily interpreted in terms of energy conservation: The first term, similarly as in Eq. (12), is the divergence in energy space of the current carried by species i . This term is balanced by energy exchange with the other species [the sum over j in Eq. (14)] and external sources (right-hand side).

We note that Eq. (14) contains no approximation so far; it is strictly equivalent to the original transport equations. It is still an integral equation, though, since the ω_i are integrals over the Ψ_j . However, it is similar in structure to the approximate Eq. (7), and one may identify the

$$\omega(E) = N \int_E^{E_0} dE' \Psi(E') \left[\int_0^E \sigma(E', T) T dT + \int_{E'-E}^{E'} \sigma(E', T) (E' - T) dT \right]. \quad (11)$$

The meaning of this quantity becomes clear by taking the derivative of $\omega(E)$. One may show that $d\omega/dE = E\Delta(E)$, therefore the balance Eq. (3) becomes

$$-\frac{d\omega}{dE} = E\delta(E - E_0). \quad (12)$$

Hence one may recognize the energy slowing down density as a current in energy space, the divergence of which is balanced by external sources. The minus sign in the above equation comes from the fact that we deal with a process of energy degradation. The energy slowing down density at zero energy, $\omega(E=0)$, is just the *deposited energy*, a quantity that is more familiar in the context of collision cascades.

In generalizing this concept to multicomponent media, i.e., introducing an ω_i for each individual species, one faces the difficulty that the two particles involved in a collision may belong to different species. Thus, it is not clear at first as to which species' ω_i such a collision even should contribute. In order that $\omega_i(E=0)$ be the energy deposited in the species i , we define $\omega_i(E)$ as the energy gained in a collision by species i below energy E in the spectrum, where before collision the moving particle may belong to any species and has an energy *above* E :

two to get the relation

$$\omega_i(E) \cong N \sum_j [c_j \sigma_{ij}^s(E) E^2 \Psi_i(E) + c_i \sigma_{ji}^r(E) E^2 \Psi_j(E)]. \quad (15)$$

It is a noteworthy fact that in both the exact relation Eq. (13) and the approximate Eq. (15), the energy slowing down density for the species i contains the fluxes of *all* species j .

The total-energy slowing down density $\omega(E) = \sum_i \omega_i(E)$ may be given in terms of the approximate Eq. (15),

$$\omega(E) \cong N E^2 \sum_{i,j} c_j \bar{\sigma}_{ij}(E) \Psi_i(E), \quad (16)$$

where we have introduced the energy slowing down cross section,

$$\bar{\sigma}_{ij} = \sigma_{ij}^s + \sigma_{ij}^r. \quad (17)$$

The value of ω is constant and equal to the bombarding energy E_0 , as follows immediately from Eq. (14). This simply expresses energy conservation and holds true as

long as losses to the electronic system may be disregarded. On the other hand, one may include inelastic effects quite naturally by regarding the electronic system as an independent species. However, in all calculations presented below we explicitly neglect electronic effects altogether, since this is not our major focus here.

IV. PARTICLE SLOWING DOWN DENSITY AND NUMBER OF RECOILS

A quantity of particular interest in collision cascades is the number of atoms participating. In other words, we are interested in the number of recoils created in a certain energy interval. This quantity will be relevant to the number of defects or damage in the target material as a consequence of the cascade. In order to conveniently calculate the number of recoils, a few auxiliary quantities will be introduced in the following.

Let $F_i(E)dE$ be the number of i atoms set in motion at energy (E, dE) due to collisions by moving atoms of any kind:

$$F_i(E) = \int_E^{E_0} dE' N c_i \sum_j \Psi_j(E') \sigma_{ji}(E', E). \quad (18)$$

This quantity is known in the literature as the recoil density.¹⁶ In analogy to the energy slowing down density, Eq. (13), we define the particle slowing down density as the average number of particles slowing down via collision from an energy $E' > E$ to an energy below E :

$$\chi_i(E) = \int_E^{E_0} dE' \Psi_i(E') N \sum_j c_j \int_{E'-E}^{E'} \sigma_{ij}(E', T) dT. \quad (19)$$

In order to avoid possible confusion, we note that the term *slowing down density* is also used in Ref. 4; however, there it denotes a different quantity, namely $\Psi_i(E)/v_i$. Our definition Eq. (19) is equivalent to the one in Ref. 15.

Differentiating Eq. (19) with respect to E and using the transport equations, Eq. (3), one obtains

$$-\frac{d\chi_i}{dE} = F_i(E) + \delta_{i1} \delta(E - E_0). \quad (20)$$

The above equation is another form to write the original transport equation. Such as Eq. (14) expresses the conservation of energy, Eq. (20) describes the balance of particles: The term on the left-hand side represents the divergence in energy space of the i -particle current, while the right-hand side contains two source terms, i.e., the recoil density F_i and external sources.

One can immediately integrate Eq. (20) to get the total number N_i of recoils generated above some displacement threshold energy E_d ,

$$N_i = \int_{E_d}^{E_0} dE F_i(E) = \chi_i(E_d) - \delta_{i1}. \quad (21)$$

The meaning of this equation is clear: The number of recoils created above energy E_d is equal to the number of atoms slowing down through this energy; the projectile is not counted among the recoils.

Equation (21) is, as it stands, not much help unless the slowing down density χ is known. It may, in principle, be

computed from Eq. (19), but this involves a double integration. With methods similar to those of Appendix A, however, a useful approximation may be obtained:

$$\chi_i(E) \cong \Psi_i(E) N \sum_j c_j S_{ij}(E). \quad (22)$$

This relationship is local in energy and involves only the stopping powers rather than the full cross sections. Thus we may compute the total number of recoils N_i directly from the particle flux Ψ_i at the displacement threshold energy.

V. SOLUTIONS

In the following, we wish to present solutions to the approximate equations obtained above. We shall compare our results with expressions available in the literature for the case of so-called power-law cross sections, but also derive an explicit solution for general-interaction laws. In all calculations below we neglect electronic interaction.

A. Monoatomic target

In a monoatomic medium, it is

$$\omega(E) = N \bar{\sigma}(E) E^2 \Psi(E) = E_0, \quad (23)$$

where we have suppressed the indices. Hence, the particle flux becomes

$$\Psi(E) = \frac{E_0}{N \bar{\sigma}(E) E^2}. \quad (24)$$

From this we obtain the particle slowing down density as

$$\chi(E) = \frac{E_0 S(E)}{E^2 \bar{\sigma}(E)}, \quad (25)$$

and by differentiation, we obtain the recoil density as

$$F(E) = K(E) \frac{E_0}{E^2}. \quad (26)$$

The quantity $K(E)$ appearing here is termed displacement efficiency,⁴ and is given by

$$K = -E^2 \frac{d}{dE} \frac{S(E)}{E^2 \bar{\sigma}(E)} \cong \frac{S(E)}{E \bar{\sigma}(E)}. \quad (27)$$

The approximation above is strictly valid for power cross sections, and we have checked that it is an underestimation by at most 20% for the Kr-C potential.

We wish to make contact with solutions available in the literature for the case of power cross sections. These approximate the scattering in a potential $V(r) \propto r^{-1/m}$ and read^{17,10}

$$d\sigma(E, T) = C_m E^{-m} T^{-1-m} dT. \quad (28)$$

For such a scattering law, the stopping cross section is given by

$$S(E) = \frac{1}{1-m} C_m E^{1-2m}, \quad (29)$$

and the energy slowing down cross section is

$$\bar{\sigma}(E) = \frac{1}{\Gamma_m(1-m)} C_m E^{-2m} = \frac{1}{\Gamma_m} \frac{S(E)}{E}, \quad (30)$$

where $\Gamma_m = m / [\psi(1) - \psi(1-m)]$, and $\psi(x)$ denotes the digamma function.¹⁸

With this, the spectrum in Eq. (24) becomes

$$\Psi(E) = (1-m)\Gamma_m \frac{E_0}{NC_m E^{2-2m}} = \Gamma_m \frac{E_0}{NC_m E S(E)}, \quad (31)$$

which is the well-known rigorous asymptotic expression of linear cascade theory.¹⁰ The recoil density results as

$$F(E) = \Gamma_m \frac{E_0}{E^2}, \quad (32)$$

with an energy independent displacement efficiency $K = \Gamma_m$. These are the exact results for power cross sections.^{16,2}

Thus, our analysis reproduces the exact asymptotic result for power-law cross sections. Moreover, it yields a simple expression for the asymptotic energy dependence of the flux for general collision cross sections, Eq. (24). In particular, we obtain that it is a *local* form of the collision cross section—more precisely, only a special moment of it, the energy slowing down cross section—which determines the asymptotic flux distribution.

Note that the distribution (24) results as a direct consequence of our discussion of energy conservation in the system, Sec. III. Since the energy slowing down density ω —which is constant and identically equal to E_0 in the case of a monoatomic target—is asymptotically proportional to the flux Ψ , the latter is proportional to E_0 . Since $\bar{\sigma}(E)$ serves as the nontrivial factor of proportionality between ω and Ψ , we call it the energy slowing down cross section.

Another result is that the displacement efficiency, a numerical factor that gives the number of recoils in a cascade, could be identified as the ratio of two moments of the cross section. These moments are the energy slowing down cross section $\bar{\sigma}$ denoting the rate at which energy is degraded, and the stopping cross sections, which are the rate at which moving atoms lose energy. The displacement efficiency is thus determined by the competition of energy degradation and particle slowing down.

B. Binary targets

The equations for recoil generation in a binary target explicitly read

$$\begin{aligned} \frac{d}{dE} [(c_1 \bar{\sigma}_{11} + c_2 \sigma_{12}^s) E^2 \Psi_1 + c_1 \sigma_{21}^r E^2 \Psi_2] \\ - c_2 S_{12} \Psi_1 + c_1 S_{21} \Psi_2 + \frac{E_0}{N} \delta(E - E_0) = 0, \\ \frac{d}{dE} [(c_2 \bar{\sigma}_{22} + c_1 \sigma_{21}^s) E^2 \Psi_2 + c_2 \sigma_{12}^r E^2 \Psi_1] \\ + c_2 S_{12} \Psi_1 - c_1 S_{21} \Psi_2 = 0, \end{aligned} \quad (33)$$

where it is assumed, as in Eq. (3), that a particle of species 1 acts as a projectile. By summing these two equations, we find the total-energy integral

$$\bar{\sigma}_1 \Psi_1 + \bar{\sigma}_2 \Psi_2 = \frac{E_0}{NE^2}, \quad (34)$$

where we introduced the total-energy slowing down cross sections $\bar{\sigma}_i$ as

$$\begin{aligned} \bar{\sigma}_1 &= c_1 \bar{\sigma}_{11} + c_2 \bar{\sigma}_{12}, \\ \bar{\sigma}_2 &= c_2 \bar{\sigma}_{22} + c_1 \bar{\sigma}_{21}. \end{aligned} \quad (35)$$

To discuss this system further, it is advantageous to introduce

$$\psi_1(\epsilon) = \frac{N}{E_0} \bar{\sigma}_1(E) E^2 \Psi_1(E), \quad (36)$$

$$\psi_2(\epsilon) = \frac{N}{E_0} \bar{\sigma}_2(E) E^2 \Psi_2(E), \quad (37)$$

with $\epsilon = E/E_0$. For a monoatomic target, $\psi(\epsilon)$ is a dimensionless constant equal to 1, cf. Eq. (23). With the abbreviations

$$\begin{aligned} s_1(\epsilon) &= \frac{c_2 S_{12}(E)}{E \bar{\sigma}_1(E)}, & r_1(\epsilon) &= \frac{c_2 \sigma_{12}^r(E)}{\bar{\sigma}_1(E)}, \\ s_2(\epsilon) &= \frac{c_1 S_{21}(E)}{E \bar{\sigma}_2(E)}, & r_2(\epsilon) &= \frac{c_1 \sigma_{21}^r(E)}{\bar{\sigma}_2(E)}, \end{aligned} \quad (38)$$

the system (33) then reads

$$\begin{aligned} \frac{d}{d\epsilon} \{ (1-r_1)\psi_1 + r_2\psi_2 \} - \frac{1}{\epsilon} s_1 \psi_1 + \frac{1}{\epsilon} s_2 \psi_2 &= -\delta(1-\epsilon), \\ \frac{d}{d\epsilon} \{ (1-r_2)\psi_2 + r_1\psi_1 \} - \frac{1}{\epsilon} s_2 \psi_2 + \frac{1}{\epsilon} s_1 \psi_1 &= 0. \end{aligned} \quad (39)$$

The energy integral is, by summation

$$\psi_1 + \psi_2 = 1. \quad (40)$$

We can express ψ_2 by ψ_1 and readily solve the remaining first-order differential equation in $(1-r_1-r_2)\psi_1$. We obtain

$$\begin{aligned} (1-r_1-r_2)\psi_1(\epsilon) &= [1-r_2(1)]h(\epsilon) \\ &+ h(\epsilon) \int_{\epsilon}^1 \left[\frac{s_2}{\epsilon'} + \frac{dr_2}{d\epsilon'} \right] \frac{d\epsilon'}{h(\epsilon')}, \\ (1-r_1-r_2)\psi_2(\epsilon) &= -r_1(1)h(\epsilon) \\ &+ h(\epsilon) \int_{\epsilon}^1 \left[\frac{s_1}{\epsilon'} + \frac{dr_1}{d\epsilon'} \right] \frac{d\epsilon'}{h(\epsilon')}, \end{aligned} \quad (41)$$

where we used the homogeneous solution

$$h(\epsilon) = \exp \left[- \int_{\epsilon}^1 \frac{s_1 + s_2}{1-r_1-r_2} \frac{d\epsilon'}{\epsilon'} \right]. \quad (42)$$

So far, the above equations refer to *self-bombardment* of a binary target, that is, when the bombarding species is one of the two constituents. This may not be the typical situation in experiments; one would rather like to have the corresponding formulas for the case that the bombarding particle is different from the target components. Indeed, the pertinent equations allow an integration in

closed form,¹⁹ but the resulting terms are rather unwieldy and will not be presented here.

C. Detailed balance

The low-energy part of a collision cascade is expected to be in an asymptotic state, which is largely independent of the initial stage. In particular, for cascades in a multicomponent medium one will assume that the energy sharing among the different species has reached some stable equilibrium situation. More specifically, one might suspect that the energy slowing down density $\omega_i(E)$ for each element levels off at some constant value, independent of the actual energy E . Such is indeed the case [cf. Eq. (15)] if the cross sections for each species i to scatter at any other species j show the same energy dependence for all j :

$$\sigma_{ij}(E) \propto \sigma_{ii}(E). \quad (43)$$

The cross sections used in Refs. 4 and 20 meet the above restriction.

Setting $d\omega_i/dE=0$ in Eq. (14) yields the condition of *detailed balance*, which for a binary medium explicitly reads

$$c_2 S_{12} \Psi_1 = c_1 S_{21} \Psi_2. \quad (44)$$

It expresses the balance of energy flow via collisions from and to each species: At any given energy, each species receives as much energy from the others as it returns back to them.

Equation (44) together with the energy conservation condition $\sum \omega_i = E_0$ allows one to solve for the fluxes $\Psi_i(E)$,

$$\Psi_1(E) = \frac{E_0}{NE^2} \frac{c_1 S_{21}(E)}{c_1 S_{21}(E) \bar{\sigma}_1(E) + c_2 S_{12}(E) \bar{\sigma}_2(E)}, \quad (45)$$

$$\Psi_2(E) = \frac{E_0}{NE^2} \frac{c_2 S_{12}(E)}{c_1 S_{21}(E) \bar{\sigma}_1(E) + c_2 S_{12}(E) \bar{\sigma}_2(E)}.$$

If the power cross sections of Andersen and Sigmund⁴ are used, Eq. (45) is identical to their Eq. (24), while Eq. (44) is equivalent to their Eq. (25). For general power cross sections, however, Eq. (45) does not represent the correct asymptotic behavior, cf. Ref. 5.

As to the restriction in Eq. (43), there is little support from realistic particle interaction laws, especially in the case of widely different masses. Its motivation rather stems from the mathematical simplifications that it introduces (cf. also the footnote on p. 8 in Ref. 4). In general, σ_{ii} and σ_{ij} will be different functions of energy, and the relative importance of intra and interparticle collisions will thus depend on energy, which impedes the energy slowing down densities to reach stationary values. Yet the detailed balance solution, Eq. (45), may serve as a useful orientation, since it avoids the necessity of solving a system of differential equations. Its quantitative accuracy will be discussed below.

VI. DISCUSSION

A. Energy partitioning in binary media

We wish to apply our theory to the bombardment of HfC. This specific target is expected to display interesting behavior, e.g., deviations from stoichiometry, since the masses and atomic numbers of the constituents are drastically different. Moreover, this system has been studied experimentally.¹¹

All calculations in this work have been performed using the Kr-C potential,²¹ for which the cross section and its moments have been obtained numerically (see Appendix B). All quantities presented below have been obtained by a numerical evaluation of Eqs. (41) using these moments of the cross section. Electronic interactions were neglected throughout.

Figure 1 shows the fraction of energy $\omega_C(E)/E_0$ carried by the C system, for various bombarding conditions. For reasons of energy conservation, the energy carried by the Hf system is given by $\omega_{Hf} = E_0 - \omega_C$. The curves represent self-bombardment at 6 and 100 keV. If the bombarding particle is C, then all energy is initially in the C system, hence $\omega_C(E)/E_0$ is equal to 1 at the bombarding energy. Conversely, $\omega_C(E)/E_0$ is equal to 0 at the bombarding energy for Hf bombardment. It is seen that all curves approach a common asymptotic equilibrium curve at low energies, regardless of the bombarding condition. Note that there is no simple equipartition of energy: The C system carries the larger portion (60%) at low energies, although the target consists of equal parts of C and Hf. Note also that the system is not strictly in a state of detailed balance, since this would require that ω_C is constant.

The fact that the carbon signal for Hf bombardment

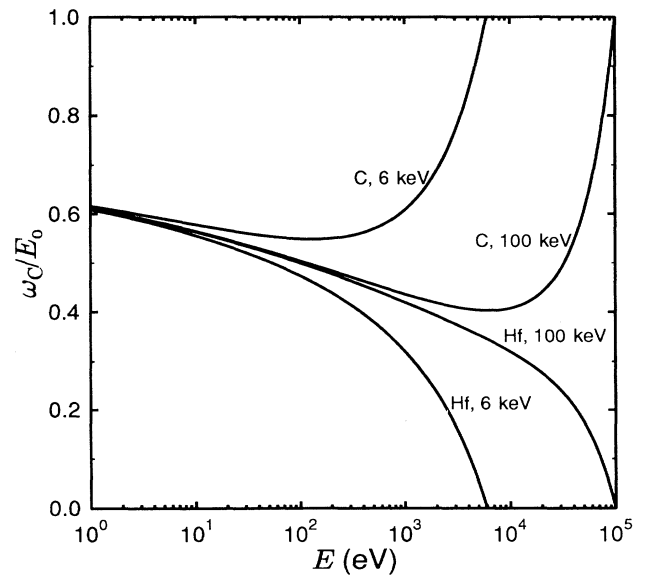


FIG. 1. Energy slowing down density of the C system in a collision cascade in HfC. The labels on the curves denote the bombarding species and energy.

extends up to the initial energy of Hf, even though the maximum energy of a C recoil is much lower, might appear disturbing. However, it is not in conflict with the definition of the energy slowing down density, Eq. (13), since $\omega_i(E)$ measures the amount of energy flowing through energy E . The situation is different for the fluxes Ψ_i , see below.

The energy slowing down density at zero energy is the energy deposited in the corresponding system, shortly called partial deposited energy. This quantity is well defined²² for a monoatomic medium (for vanishing electronic losses it is simply $\omega(E)=E_0$), but certainly merits some comment for the case of a compound. First of all, from Fig. 1 it is not clear that there is actually a well defined limit $\omega_i(E \rightarrow 0)$. On the other hand, it would be meaningless to extend the present calculation to energies below 1 eV, since the binary collision assumption underlying the transport Eq. (3) would long be violated for such low energies. Eventually, all energy will thermalize and there will be equipartition among all degrees of freedom. The path towards this equilibrium, however, begins with a linear, collisional stage, which is described by the present scheme and extends down to somewhere in the lower eV region. It is therefore reasonable to regard the partitioning of energy at the end of this linear stage, which we take—somewhat arbitrarily—at 10 eV. Thus we show in Fig. 2(a) the partial deposited energy in a hypothetical $\text{Hf}_{1-x}\text{C}_x$ compound. The incoming ion is Hf at 100 keV. At this energy, however, the low-energy part of the cascade is already in its asymptotic state and independent of the bombarding condition, as can be seen from Fig. 1. The dotted lines in Fig. 2(a) correspond to a stoichiometric partitioning, and the dashed curves correspond to the detailed balance solution, Eq. (45). It is observed that the C species receives more energy than according to stoichiometry at the cost of the Hf species. This preferentiality of the lighter species may be understood qualitatively within the concept of detailed balance. However, the magnitude of the effect is overestimated by the detailed balance solution.

Partial deposited energies have been calculated previously for the TaO system.⁶ The authors did so by using backward equations. In this approach one has to impose boundary conditions at zero energy. These, however, cannot be determined uniquely without anticipating the result. This problem appears to be closely related with the fact that $\omega_i(E)$ need not have a well defined limit for $E \rightarrow 0$.

Regardless of the details, the authors of Ref. 6 find that more energy is deposited in the heavier species Ta, opposite to our case. The discrepancy may be traced back to the different input used: In Ref. 6, the Thomas-Fermi cross section was used, which is less realistic at low energies compared to the Kr-C interaction used here. If their cross sections are used in our formula (45), their result is qualitatively reproduced.

Although the energy slowing down density—or its value at low energies—may be an intuitive concept to quantify the partitioning of energy in a collision cascade, it is not directly accessible to measurement. Observable quantities of interest are, e.g., sputtered particle fluxes

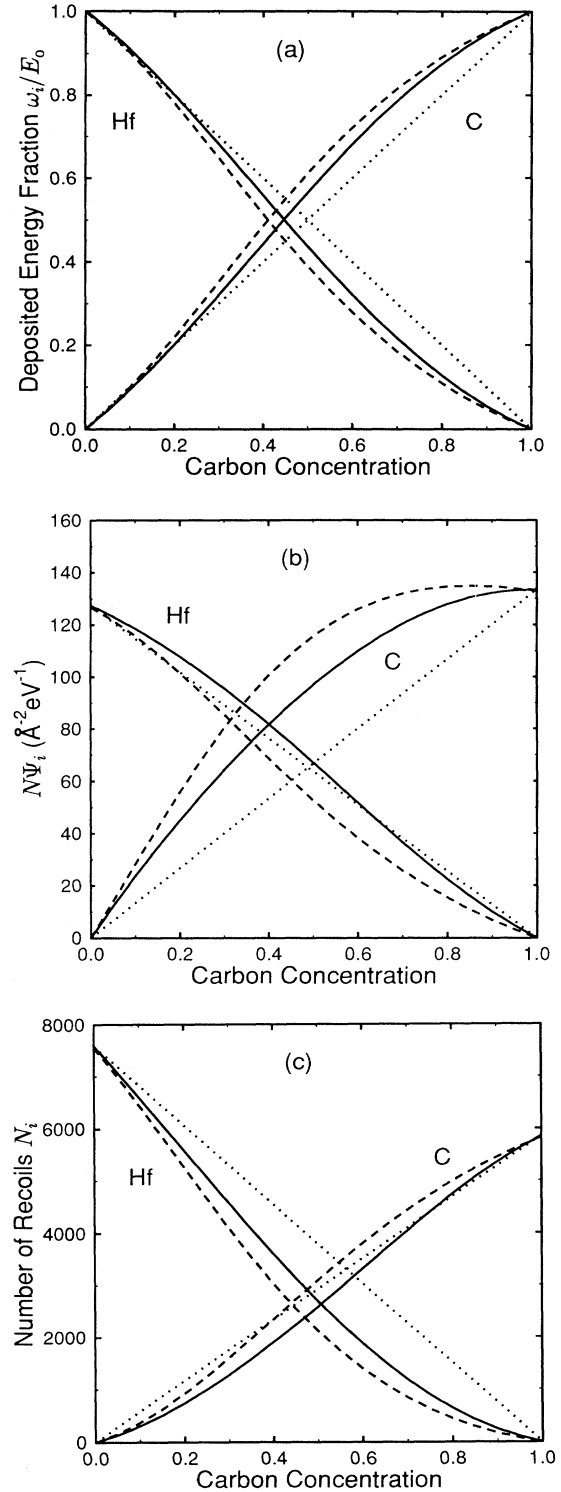


FIG. 2. Energy partitioning in a collision cascade, initiated by 100 keV Hf, in the hypothetical medium $\text{Hf}_x\text{C}_{1-x}$ as a function of C concentration. Solid lines: Eqs. (41). Dashed lines: Detailed balance solution, Eq. (45). The dotted lines denote stoichiometric behavior as a reference. (a) Energy fraction deposited in low-energy (< 10 eV) recoil motion, $\omega_i(E=10 \text{ eV})/E_0$. (b) Low-energy particle flux $\Psi_i(E=10 \text{ eV})$. (c) Number of recoils N_i , generated above 10 eV in the cascade.

and the damage in the irradiated material. These are directly related to the fluxes Ψ_i and the number of recoils N_i , which we display in Figs. 2(b) and 2(c), respectively. Both figures show a more pronounced deviation from stoichiometry than Fig. 2(a). In Fig. 2(b), the C flux shows a clear overstoichiometric behavior, whereas the Hf flux is nearly stoichiometric. Again, the preferentiality is qualitatively well described (although exaggerated) by the detailed balance solution (dashed lines); however, the Hf flux is suppressed to understoichiometric values by this approximation. We note that for detailed balance, the flux ratio is determined by Eq. (44), which in the case of power cross sections yields $\Psi_1/\Psi_2 = c_1/c_2(M_2/M_1)^{2m}$. The factor $(M_2/M_1)^{2m}$ represents the preferentiality of the lighter species; this constitutes the main effect observed in Fig. 2(b). Results like those of Fig. 2(b) have been found in Ref. 4; there, however, both the light *and* the heavy constituents showed overstoichiometric behavior.

In contrast, Fig. 2(c) shows an understoichiometric behavior for the number of recoils of both species. This may be explained by the large mass difference between Hf and C: In interparticle collisions, a larger amount of energy is spent in subthreshold collisions and is thus not available for recoil production. The effect is more pronounced for the heavy species Hf than for C, which may be attributed to the general preferentiality of the light species. Understoichiometric behavior has also been found for recoil densities in Ref. 4. At equal concentrations, our results show similar recoil numbers for both species. This is different from the results of Refs. 7 and 8, where the heavy atoms are found to be displaced preferentially. This discrepancy is due to the choice of 10 eV for the displacement threshold energies used in our study, while Refs. 7 and 8 assume a much larger value, around 60 eV. It may be seen from Fig. 1, and it is also shown in Ref. 8, that at higher energies, the partitioning is more in favor of the heavier species. Note, however, that the two curves in Fig. 2(c) rely on the somewhat arbitrary assumption of equal displacement threshold energies for both species. In practice this is generally not the case, which means that the recoil numbers in Fig. 2(c) should only be regarded as a model study. Even more important is the fact that the displacement threshold energies themselves may depend on composition,^{12,23} which is an additional possible source for nonstoichiometric behavior.

B. Comparison to simulations and experiment

In order to check our analytical results we performed a number of Monte Carlo computer simulations. The Monte Carlo code was specifically designed to solve the system of transport equations (3); details may be found in Refs. 24, 25, and 5.

In Figs. 3(a) and 3(b) the special case of 6 keV self-bombardment of HfC is treated. Kr-C interaction²¹ was assumed, and electronic effects were ignored. The simulation was performed without spatial resolution, and no surface or bulk binding was applied. The agreement between analytical theory and the simulational solution is excellent over almost the entire range of energies. Even

for energies close to the bombarding energy the present analytical theory gives a surprisingly good description of the spectra. The figures also contain spectra that refer to a situation of detailed balance, Eq. (45). The spectra are found to deviate quite markedly at high energies, and converge for low energies slowly towards the simulated spectra. The asymptotic slope fits quite well, but the relative height of the curves deviates by around 20% from the exact solution. We hence conclude that detailed balance is only established at very small energies. Nevertheless, detailed balance is an intuitive concept that may be used to understand the qualitative features of the particle spectra even for this case of drastically different masses.

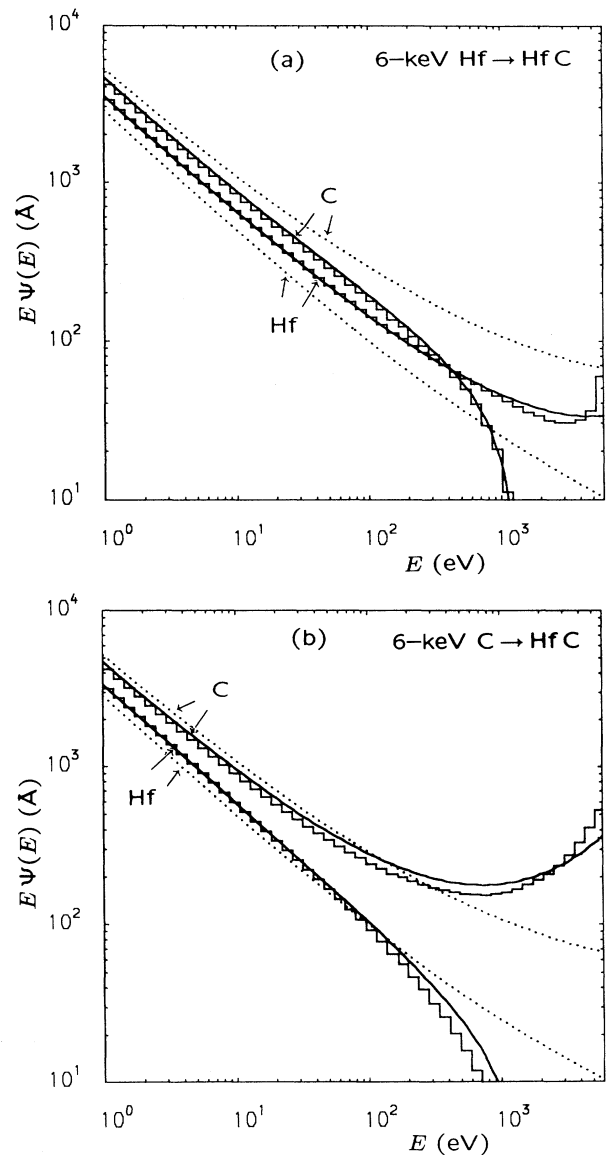


FIG. 3. Energy distributions of recoils in a HfC compound, induced by a 6 keV C (a) and Hf (b) atom. Histogram: Monte Carlo simulation. Lines: Eqs. (41). Dots: Detailed balance solution, Eq. (45).

Quantitatively, the preferentiality of the lighter species is overestimated by detailed balance.

It is interesting to see how the energy spectrum depends on the composition of the medium. Evidently, one would expect the most pronounced effects for the case where one component is diluted. Then, the cascade is governed primarily by collisions among the majority species, a situation termed *dominance* in Ref. 5. Figure 4 shows for the hypothetical compound $\text{Hf}_x\text{C}_{1-x}$ the flux of C recoils due to an impact of a 6 keV Xe atom. The histograms represent a simulation in an infinite medium, ignoring binding forces and electronic effects. In the case where Hf is the majority constituent, $x=0.99$, the spectrum is notably flatter than in the reverse case, $x=0.01$. The reason for this behavior is found in the fact that C-C collisions are characterized by a softer part of the Kr-C potential [or smaller Lindhard energy E_L , Eq. (B2)]. To be more quantitative, one may assign to the Kr-C cross section a local power exponent m , which is defined according to Eq. (29) via

$$1-2m = \frac{d \ln S(E)}{d \ln E} . \quad (46)$$

For C-C collisions at 10 eV interaction energy, Eq. (46) gives $m=0.23$. As a reference we included in Fig. 4 a straight dashed line with a slope according to Eq. (31) using this m value. The slope of the C spectrum for $x=0.01$ coincides very well with this reference.

Hf-Hf collisions, on the other hand, are represented by a smaller value for m . The same holds true for Hf-C and, to a smaller degree, for C-Hf collisions. In a Hf-rich environment where the collision cascade is dominated by

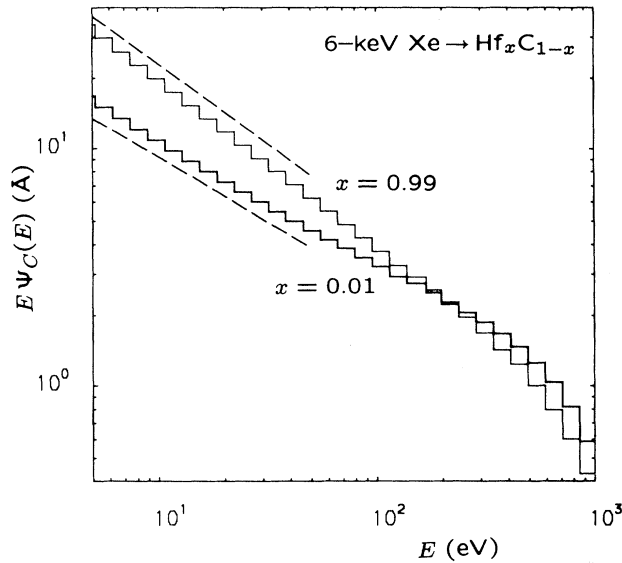


FIG. 4. Simulated energy distributions of C recoils in a (hypothetical) $\text{Hf}_x\text{C}_{1-x}$ compound, induced by a 6 keV Xe atom, for the two extreme cases $x=0.01$ and $x=0.99$. The distribution for $x=0.99$ has been amplified by a factor of 100. The dashed lines represent the slopes predicted by an asymptotic theory (Ref. 5) (see text).

Hf-Hf collisions, C atoms are primarily set in motion by Hf-C collisions and it must be expected that the C spectrum is thus steeper, i.e., characterized by a smaller effective m value. This is indeed observed in Fig. 4. Rigorous analysis of this phenomenon based on power-law interaction⁵ predicts that in a Hf-rich environment, the C spectrum behaves asymptotically like $1/E^{2-2(m_{\text{HfHf}}+m_{\text{CHf}}-m_{\text{HfC}})}$; for 10 eV interaction energy, the exponents read

$$m_{\text{HfHf}}=0.12, \quad m_{\text{CHf}}=0.17, \quad m_{\text{HfC}}=0.13, \quad (47)$$

and hence Ref. 5 predicts an effective value of

$$m = m_{\text{HfHf}} + m_{\text{CHf}} - m_{\text{HfC}} = 0.16 .$$

The upper dashed line in Fig. 4 corresponds to this value, and its slope indeed agrees very well with the one of the simulated C spectrum for $x=0.99$.

We note that these local values for the power exponent m also account for the slope of the Hf and C spectra displayed in Figs. 3 for a HfC compound. As shown above, the slope of the spectrum is well described by the detailed balance solution. For power-law interaction, the Hf spectrum should follow a $1/E^{2-2m_{\text{HfC}}}$ distribution, and the C spectrum a $1/E^{2-2m_{\text{CHf}}}$ distribution.⁵ In view of the almost identical values for $m_{\text{HfC}} \approx m_{\text{CHf}}$, the finding that the C and Hf spectra are nearly parallel (see Figs. 3) is in good agreement with this prediction.

In Fig. 5, we plot calculated energy distribution of sputtered particles for a HfC compound bombarded by a 6 keV Xe atom, and compare them to distributions from an experiment by Szymonsky.¹¹ Again, Kr-C interaction cross sections have been assumed, still without electronic effects. In this case the full spatial dependence was considered in the simulation (histogram), and a planar surface binding with binding energies of 6.7 eV for Hf and

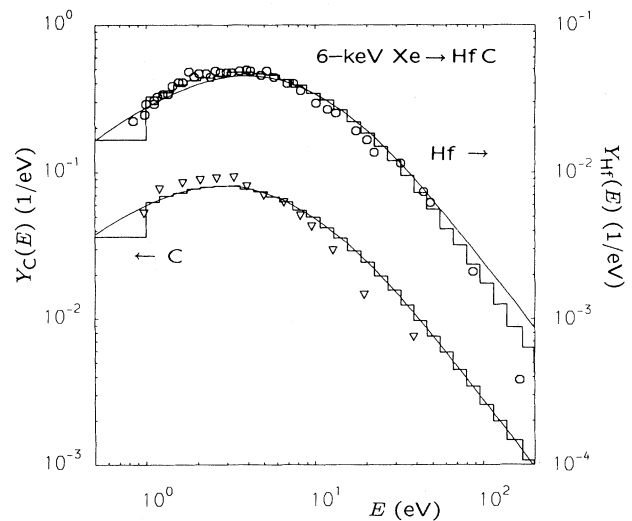


FIG. 5. Energy spectra $Y(E)$ of particles sputtered from a HfC target by 6 keV Xe bombardment. Smooth curves: present theory. Symbols: experiment (Ref. 11). Histograms: Monte Carlo simulation.

4.8 eV for C was assumed. The particular values for the binding energies were motivated by a fit to the experimental energy distributions.¹¹ In the analytical calculation (smooth curves in Fig. 5), spatial dependence was not considered; the corresponding spectra represent spatial averages, which have been transformed in the common way²⁶ to account for a planar surface binding. The absolute magnitude of the analytically obtained spectra has been adjusted so that they coincide with the simulation at 10 eV. Since the experimental spectra are available only in arbitrary units, they have been adjusted as well to give the same height as the simulation data.

It is observed that the analytical spectra are very close to the simulations; slight deviations, however, occur for the Hf spectrum, which must have their origin in the spatial dependence. Also experiment and simulation agree fairly well, perhaps with some slight deviation in the position of the maximum of the C spectrum. In particular, the experiment shows a similar slope at high energies for the two spectra, which is largely confirmed by the theoretical curves. This conclusion coincides with the observation made in Figs. 3 that Hf and C spectra are proportional to each other over a wide range of recoil energies.

There exists another measurement of sputtered particle energy spectra in a compound.¹² The authors bombarded a NiW-alloy sample and made a careful effort to resolve different slopes in the sputtered fluxes for the individual species, as suggested by the theory of Andersen and Sigmund,⁴ but again, no such effect could be observed.

A difference in the energy distributions of sputtered particles such as the ones displayed in Fig. 4 might be observable experimentally. We therefore propose to measure sputtered particle spectra for compounds $A_x B_{1-x}$ with, respectively, $x \ll 1$ and $1-x \ll 1$, and widely differing masses of the constituents A and B. These spectra should show notable differences in their slopes.

There are a number of effects not considered in this work that may be important in the real situation. First of all, spatial dependence has been disregarded altogether. There is reason to believe that this may be substantial for the understanding of preferential sputtering,⁴ since sputtering occurs mainly from the outermost layer and is thus quite sensitive to the spatial arrangement of the cascade.

Thus, the comparison of the measured spectra with our theory should be considered with some caution. Electronic stopping might have an influence on the sputtered spectra, in particular in the case of C. One should also bear in mind that the measured data were taken at high fluence where the concentrations in the target, especially in regions close to the surface, might have been altered during bombardment. It appears likely that C, being the lighter component and having the smaller surface binding energy, was depleted near the surface. Another source of uncertainty may arise from the target structure, which may affect the collision probabilities for the two species. Thus, Robinson²⁷ showed that short-range order in a compound may have an effect on recoil densities. In the system studied there, the "caging" of a small light species by a big and heavy species shields the light species some-

what from collisions. Such effects are not included in our theory, which assumes a structureless medium.

VII. CONCLUSIONS

We presented an analytical method to derive the energy distributions in a collision cascade in a multicomponent medium. The method follows the spirit of the age theory, which is well known in neutron- and electron-transport theory.^{13,14} In essence, the integral transport equations are converted to differential equations by Taylor expansion in the appropriate variable. A similar method also gives useful results for the slowing down and reflection of a (light) projectile from a solid surface.²⁸

The results obtained contain only certain moments of the interaction cross sections: The well-known stopping cross sections $S_{ij}(E)$ and the energy slowing down cross sections, which are introduced here. Unlike in earlier treatments,⁴ there are no restrictions in the present study on the form of the interaction potential between particles; for Kr-C interaction, the necessary moments are given in Appendix B. For elemental and binary targets, the energy distribution of recoils in the collision cascade is expressed analytically with the help of these moments.

Electronic interaction can be formally included within the present framework. The results presented in this work, however, neglect electronic effects.

The present scheme is applied to the calculation of collision cascades in binary media, where $Hf_x C_{1-x}$ is taken as a case study. There are several possible ways to quantify deviations from stoichiometric behavior, and it turns out that the results depend on the quantity considered. Thus, the energy of the initiating particle is deposited in the course of the cascade preferentially into low-energy motion of the C species. Likewise, the flux of low-energy particles is overstoichiometric for C and is nearly stoichiometric for Hf. On the other hand, the number of recoils generated in the cascade is understoichiometric for both species, the effect being more pronounced for Hf.

Comparison of our analytical results with Monte Carlo simulations shows excellent agreement in the entire regime of recoil energies, with minor deviations near the bombarding energy.

The energy distributions of recoils of the individual species in a binary medium is different from the respective spectra of the pure media. Interspecies collisions tend to equalize the slopes of the two spectra. This is also found in another theoretical study based on power-law interaction potentials,⁵ and is confirmed by experiment.^{12,11}

Different slopes of the energy spectrum are found, however, for different compositions of a binary medium. Here, the systematics is such that the majority species dictates the behavior. Thus, the spectrum becomes flatter if the light species is more abundant, and vice versa. The differences might be observable experimentally, and it is proposed to perform such an experiment.

ACKNOWLEDGMENTS

We thank P. Sigmund for critical comments on the manuscript. Financial support by the Deutsche Forschungsgemeinschaft is acknowledged.

APPENDIX A

We present the details of the Taylor expansion of the system of integral equations (3). The analysis is performed in several steps. First, the cross section $\sigma(E, T)$ may be transformed to the relative energy transfer $\tau = T/E$, writing

$$\sigma(E, T)dT = \sigma(E, \tau)d\tau. \quad (\text{A1})$$

Hence the loss term simply transforms as

$$dT c_j \sigma_{ij}(E, T) \Psi_i(E) = d\tau c_j \sigma_{ij}(E, \tau) \Psi_i(E). \quad (\text{A2})$$

In the scatter term, we use the relative energy variable $\tau = T/(E+T)$, which gives

$$\sigma(E+T, T)dT = \sigma(E+T, \tau) \frac{E+T}{E} d\tau. \quad (\text{A3})$$

Hence the scatter term transforms to

$$dT c_j \sigma_{ij}(E', T) \Psi_i(E') = d\tau c_j \sigma_{ij}(E', \tau) \frac{E'}{E} \Psi_i(E'),$$

$$E' = \frac{E}{1-\tau}. \quad (\text{A4})$$

In the recoil term we take $\tau = E/(E+T)$ as the relative energy variable, and get

$$\sigma(E+T, E)dT = \sigma(E+T, \tau) \frac{E+T}{E} d\tau. \quad (\text{A5})$$

Thus the recoil term transforms as

$$dT c_i \sigma_{ij}(E'', E) \Psi_j(E'') = d\tau c_i \sigma_{ji}(E'', \tau) \frac{E''}{E} \Psi_j(E''),$$

$$E'' = \frac{E}{\tau}. \quad (\text{A6})$$

Collecting terms, we finally have

$$\Delta_i(E) = N \sum_j \int d\tau \left\{ c_j \sigma_{ij}(E', \tau) \frac{E'}{E} \Psi_i(E') \right. \\ \left. + c_i \sigma_{ji}(E'', \tau) \frac{E''}{E} \Psi_j(E'') \right. \\ \left. - c_j \sigma_{ij}(E, \tau) \Psi_i(E) \right\}. \quad (\text{A7})$$

Next introduce as the logarithmic energy variable the lethargy u ,

$$E = E_0 e^{-u}, \quad (\text{A8})$$

which increases monotonically with decreasing particle energy. We keep, for the sake of simplicity, the same letters for the functions of the new variable, i.e., we write

$$\Psi(u) = \Psi(E(u)) = \Psi(E_0 e^{-u}), \quad (\text{A9})$$

and analogously for the cross section and the balance of collisions. We obtain

$$\Delta_i(E) = N \sum_j \int d\tau \{ c_j \sigma_{ij}(u', \tau) e^{u-u'} \Psi_i(u') \\ + c_i \sigma_{ji}(u'', \tau) e^{u-u''} \Psi_j(u'') \\ - c_j \sigma_{ij}(u, \tau) \Psi_i(u) \}. \quad (\text{A10})$$

Here, it is $e^{u'-u} = 1-\tau$ and $e^{u''-u} = \tau$. Now we perform a Taylor expansion in the lethargy:

$$c_j \sigma_{ij}(u', \tau) e^{-2u'} \Psi_i(u') + c_i \sigma_{ji}(u'', \tau) e^{-2u''} \Psi_j(u'') \\ = c_j \sigma_{ij}(u, \tau) e^{-2u} \Psi_i(u) + c_i \sigma_{ji}(u, \tau) e^{-2u} \Psi_j(u) \\ + (u'-u) \frac{\partial}{\partial u} [c_j \sigma_{ij}(u, \tau) e^{-2u} \Psi_i(u)] \\ + (u''-u) \frac{\partial}{\partial u} [c_i \sigma_{ji}(u, \tau) e^{-2u} \Psi_j(u)]. \quad (\text{A11})$$

This point needs some justification, since it constitutes the main approximation introduced in the present study. The expansion with respect to u' is easily accepted. Note that $u'-u$ is the lethargy increase for the colliding particle; hence it is typically small, since the cross section favors small energy transfer. This is different for u'' . However, as the dependent variable that is expanded is essentially the energy slowing down density, the variation with energy will be small (for a monoatomic, elastic collision cascade it is constant altogether). For power cross sections, one can show that this expansion yields the leading terms in an asymptotic series,⁵ i.e., for energies well below the bombarding energy. For general cross sections, as they are the major focus here, there is support for the above expansion from comparisons with pertinent simulations (cf. Sec. VI B).

From Eq. (A11) we obtain

$$\Delta_i(u) = N \sum_j \int d\tau \left\{ c_j \sigma_{ij}(u, \tau) [e^{u'-u} - 1] \Psi_i(u) + c_i \sigma_{ji}(u, \tau) e^{u''-u} \Psi_j(u) \right. \\ \left. + (u'-u) e^{u+u'} \frac{\partial}{\partial u} [c_j \sigma_{ij}(u, \tau) e^{-2u} \Psi_i(u)] \right. \\ \left. + (u''-u) e^{u+u''} \frac{\partial}{\partial u} [c_i \sigma_{ji}(u, \tau) e^{-2u} \Psi_j(u)] \right\}. \quad (\text{A12})$$

Here, the τ integrations can be performed. Note that

$$u' - u = \ln(1 - \tau), \quad u'' - u = \ln\tau \quad (\text{A13})$$

are functions of τ only. It is

$$\begin{aligned} \int d\tau \sigma_{ij}(u, \tau) e^{u'' - u} &= - \int d\tau \sigma_{ij}(u, \tau) (e^{u' - u} - 1) \\ &= \int d\tau \tau \sigma_{ij}(u, \tau) \\ &= \frac{1}{E} \int dT T \sigma_{ij}(E, T) = \frac{1}{E} S_{ij}(E, T), \end{aligned} \quad (\text{A14})$$

with the stopping cross sections $S_{ij}(E)$, Eq. (8). We furthermore introduce the following moments of the cross section (called partial energy slowing down cross sections)

$$\begin{aligned} \sigma_{ij}^s(u) &= - \int d\tau (1 - \tau) \ln(1 - \tau) \sigma_{ij}(u, \tau), \\ \sigma_{ji}^r(u) &= - \int d\tau \tau \ln\tau \sigma_{ji}(u, \tau), \end{aligned} \quad (\text{A5})$$

which have been written down in the energy variable in Eqs. (9) and (10). Then, finally, we obtain the approximate form of the transport equations, Eqs. (7).

Note that however innocuous the introduction of the energy slowing down cross section (A15) looks, the necessary interchange of differentiation and integration actually is only approximately possible, since the integration limit in the gain term depends on energy.

As a result of our analysis, the integral transport equations are transformed to a system of differential equations, Eqs. (7).

APPENDIX B

Interatomic potentials $V(r)$ used in collision cascade calculations often obey Thomas-Fermi scaling.^{17,2} This implies that a single length scale, the screening length

$$a = 0.8853 a_0 (\sqrt{Z_1} + \sqrt{Z_2})^{-2/3}, \quad (\text{B1})$$

with Bohr's radius a_0 , characterizes the interaction. Then a natural energy scale called the Lindhard energy E_L exists,

$$E_L = \frac{M_1 + M_2}{M_2} \frac{Z_1 Z_2 e^2}{a}. \quad (\text{B2})$$

In these expressions, M and Z denote the mass and atomic charge of the two interacting atoms, and e is the ele-

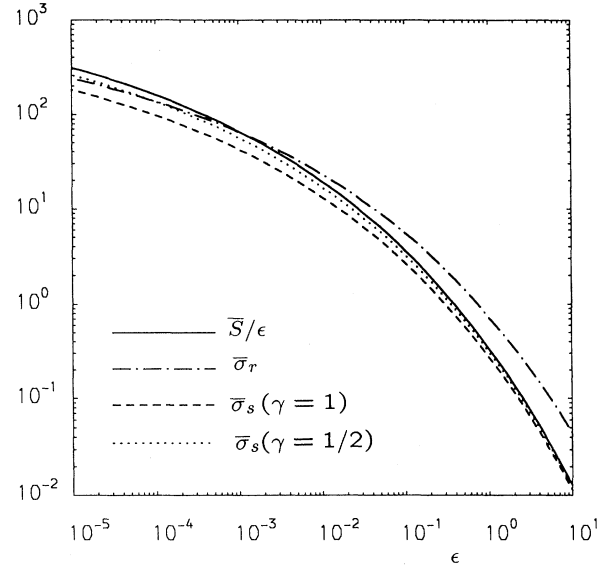


FIG. 6. Scaled cross sections (see text) for a Kr-C interaction potential as a function of reduced energy $\epsilon = E/E_L$.

mentary charge. The index 1 denotes the moving particle, while the index 2 stands for the particle at rest before the collision.

For such potentials, the stopping power may be written in reduced form as

$$S(E) = \gamma \pi a^2 E_L \bar{S}(\epsilon). \quad (\text{B3})$$

Here, \bar{S} is a universal function of $\epsilon = E/E_L$. Similarly, the partial slowing down cross sections may be reduced to universal functions,

$$\sigma^s(E, \gamma) = \gamma \pi a^2 \bar{\sigma}^s(\epsilon, \gamma), \quad (\text{B4})$$

$$\sigma^r(E, \gamma) = \gamma \pi a^2 \bar{\sigma}^r(\epsilon, \gamma). \quad (\text{B5})$$

Here, the scaled functions depend on the two variables ϵ and γ . By definition, we can decompose $\bar{\sigma}^r$ further into

$$\bar{\sigma}^r(\epsilon, \gamma) = \bar{\sigma}^r(\epsilon) + \ln(1/\gamma) \bar{S}(\epsilon)/\epsilon, \quad (\text{B6})$$

where $\bar{\sigma}^r(\epsilon) = \bar{\sigma}^r(\epsilon, \gamma = 1)$. The function $\bar{\sigma}^s(\epsilon, \gamma)$ cannot be reduced further. Note, however, that it satisfies the inequality $\bar{\sigma}^s(\epsilon, \gamma) < \bar{S}(\epsilon)/\epsilon$, and in the limit of very different masses, it is $\lim_{\gamma \rightarrow 0} \bar{\sigma}^s(\epsilon, \gamma) = \bar{S}(\epsilon)/\epsilon$. Figure 6 shows the scaled cross sections for a Kr-C interaction potential.

¹J. Lindhard, V. Nielsen, M. Scharff, and P. V. Thomsen, K. Dan. Vidensk. Selsk. Mat. Fys. Medd. **33**, No. 10 (1963).

²P. Sigmund, Rev. Roum. Phys. **17**, 823 (1972); **17**, 969 (1972); **17**, 1079 (1972).

³W. Huang, H. M. Urbassek, and P. Sigmund, Philos. Mag. A **52**, 753 (1985).

⁴N. Andersen and P. Sigmund, K. Dan. Vidensk. Selsk. Mat. Fys. Medd. **39**, No. 3 (1974).

⁵H. M. Urbassek and U. Conrad, Nucl. Instrum. Methods B **69**, 413 (1992).

⁶Y. Matsutani and S. Ishino, J. Appl. Phys. **48**, 1822 (1977).

⁷D. M. Parkin, Nucl. Instrum. Methods B **46**, 26 (1990).

⁸I. Koponen, Nucl. Instrum. Methods B **59/60**, 41 (1991).

⁹P. Agnew, Nucl. Instrum. Methods B **65**, 305 (1992).

¹⁰P. Sigmund, in *Sputtering by Particle Bombardment I*, edited by R. Behrisch (Springer, Berlin, 1981), p. 9.

¹¹M. Szymonski, Phys. Lett. **82A**, 203 (1981).

¹²H. Oechsner and J. Bartella, in *Proceedings of the VII International Conference on Atomic Collisions in Solids*, edited by J. V. Bulgakov and A. S. Tulinov (Moscow State University

- Publishing House, Moscow, 1980), p. 55.
- ¹³H. A. Bethe, M. E. Rose, and L. P. Smith, Proc. Am. Philos. Soc. **78**, 573 (1938).
- ¹⁴R. E. Marshak, Rev. Mod. Phys. **19**, 185 (1947).
- ¹⁵M. M. R. Williams, Prog. Nucl. Energy **3**, 1 (1979).
- ¹⁶P. Sigmund, Appl. Phys. Lett. **14**, 114 (1969).
- ¹⁷J. Lindhard, V. Nielsen, and M. Scharff, K. Dan. Vidensk. Selsk. Mat. Fys. Medd. **36**, No. 10 (1968).
- ¹⁸*Handbook of Mathematical Functions*, edited by M. Abramowitz and I. A. Stegun (National Bureau of Standards, Washington, DC, 1965).
- ¹⁹U. Conrad, Ph.D. thesis, Technische Universität Braunschweig, 1992.
- ²⁰M. D. Kostin, J. Appl. Phys. **37**, 3801 (1966).
- ²¹W. D. Wilson, L. G. Haggmark, and J. P. Biersack, Phys. Rev. B **15**, 2458 (1977).
- ²²K. B. Winterbon, P. Sigmund, and J. B. Sanders, K. Dan. Vidensk. Selsk. Mat. Fys. Medd. **37**, No. 14 (1970).
- ²³M. Szymanski, Appl. Phys. **23**, 89 (1980).
- ²⁴M. Vicanek and H. M. Urbassek, Nucl. Instrum. Methods B **30**, 507 (1988).
- ²⁵U. Conrad and H. M. Urbassek, Nucl. Instrum. Methods B **61**, 295 (1991).
- ²⁶M. W. Thompson, Philos. Mag. **18**, 377 (1968).
- ²⁷M. T. Robinson, Phys. Rev. B **27**, 5347 (1983).
- ²⁸M. Vicanek and H. M. Urbassek, Phys. Rev. B **44**, 7234 (1991).